Inorg. Chem. **2002**, *41*, 7006–7014

Synthesis and X-ray Crystal Structure Determination of the First Copper(II) Complexes of Tetraazamacrocycle–Glyoxal Condensates

Timothy J. Hubin,*[,†,‡] Nathaniel W. Alcock,[§] Lawrence L. Seib,[†] and Daryle H. Busch[†]

Chemistry Departments, University of Kansas, Lawrence, Kansas 66045, and University of Warwick, Coventry CV4 7AL, England

Received June 6, 2002

Novel Cu^{II} complexes $CuLCl_2$ (L = **1**–**4**) have been synthesized containing the metal bound to a well-known type of tetracyclic bisaminal formed from the condensation of glyoxal and tetraazamacrocycles (**1** = cyclam–glyoxal condensate, **2** = [13]aneN4–glyoxal condensate, **3** = cyclen–glyoxal condensate, **4** = isocyclam–glyoxal condensate). The four-coordinate complexes were characterized by X-ray crystallography, electronic spectroscopy, solid-state magnetic moments, and electron spin resonance spectroscopy. The tetracyclic bisaminals, although having four potential donor atoms, are bound in a *cis*-bidentate fashion to Cu^{II} with two additional *cis*-chloride donors. The ligands take up folded conformations, and with the exception of ligand **4**, only nonadjacent nitrogen atoms coordinate. As expected, ligand **2** in Cu(**2**)Cl_2 has a folded structure similar to those of the previously characterized **1** and **3**. The conformation of **4** in the complex Cu(**4**)Cl_2 differs from **1**–**3** in that three nitrogens direct their lone pairs to one side of the folded tetracycle, with adjacent nitrogen atoms coordinated to Cu^{II}. This difference is probably caused by the presence of the more flexible seven-membered ring rather than the five- to six-membered rings in **1**–**3**. Air oxidation of Cu^{I} in the presence of **1** or **3** results in bis(μ-hydroxo) dimers as characterized by X-ray crystal structures, suggesting dioxygen binding, followed by O–O bond splitting to give the Cu_2O_2 diamond core.

Introduction

Copper(I) and Copper(II) complexes of rigid bidentate amine ligands have recently gained attention in the modeling of multinuclear copper enzyme active sites.[1,2] This ligand type, along with the more prevalent tridentate ligands of Kitajima[3,4] and Tolman,[5,6] have been used to study the oxidation of their Cu^{I} complexes to produce Cu^{II} or Cu^{III} μ-hydroxo-, μ-oxo-, or μ-peroxo-bridged dimers or even trimers[1] that mimic active site geometries or reactivities. With this recent work in mind, and to broaden the range of metal ions which can coordinate the tetracyclic bidentate ligands formed from tetraazamacrocycle−glyoxal condensation, we have prepared and characterized Cu^{II} complexes of the series of tetracyclic bisaminals **1**−**4** (**1** = *cis*-decahydro-3a,5a,8a,-10a-tetraazapyrene, **2** = *cis*-decahydro-3a,5a,7a,9a-tetraazacyclopent[*gh*]phenalene, **3** = *cis*-decahydro-2a,4a,6a,8a-tetraazacyclopent[*fg*]acenaphthylene, **4** = *cis*-decahydro-2a,4a,7a,10a-tetraazanaphth[2,1,8-*c*,*d*,*e*]azulene) (Figure 1).

Tetracyclic bisaminals formed from simple tetraazamacrocycles condensed with glyoxal are well-known.[7−12] Each

* Corresponding author. E-mail: hubint@mcpherson.edu.
† University of Kansas.
‡ Present address: Department of Natural Science, McPherson College, McPherson, KS 67460.
§ University of Warwick.

(1) Cole, A. P.; Root, D. E.; Mukherjee, P.; Solomon, E. I.; Stack, T. D. P. *Science* **1996**, *273*, 1848.
(2) DuBois, J. L.; Mukherjee, P.; Collier, A. M.; Mayer, J. M.; Solomon, E. I.; Hedman, B.; Stack, T. D. P.; Hodgson, K. O. *J. Am. Chem. Soc.* **1997**, *119*, 8578.
(3) Kitajima, N.; Fujisawa, K.; Fujimoto, C.; Moro-oko, Y.; Hashimoto, S.; Kitagawa, T.; Toriumi, K.; Nakamura, A. *J. Am. Chem. Soc.* **1992**, *114*, 1277.
(4) Kitajima, N.; Moro-oko, Y. *Chem. Rev.* **1994**, *94*, 737.
(5) (a) Halfen, J. A.; Mahapatra, S.; Wilkinson, E. C.; Kaderli, S.; Young, V. G., Jr.; Que, L., Jr.; Zuberbuhler, A. D.; Tolman, W. B. *Science* **1996**, *271*, 1397. (b) Mahaptra, S.; Halfen, J. A.; Wilkinson, E. C.; Pan, G.; Wang, X.; Young, V. G., Jr.; Cramer, C. J.; Que, L., Jr.; Tolman, W. B. *J. Am. Chem. Soc.* **1996**, *118*, 11555.
(6) Tolman, W. B. *Acc. Chem. Res.* **1997**, *30*, 227.
(7) Caulkett, P. W. R.; Greatbanks, D.; Turner, R. W.; Jarvis, J. A. *J. Chem. Soc., Chem. Commun.* **1977**, 150.
(8) Alcock, N. W.; Moore, P.; Mok, K. F. *J. Chem. Soc., Perkin Trans. 2* **1980**, 1186.
(9) Weisman, G. R.; Ho, S. C. H.; Johnson, V. *Tetrahedron Lett.* **1980**, *21*, 335.
(10) Kolinski, R. A.; Riddell, F. G. *Tetrahedron Lett.* **1981**, *22*, 2217.
(11) Müller, R.; von Philipsborn, W.; Schleifer, L.; Aped, P.; Fuchs, B. *Tetrahedron* **1991**, *47*, 1013.

10.1021/ic020386+ CCC: $22.00
Published on Web 12/05/2002

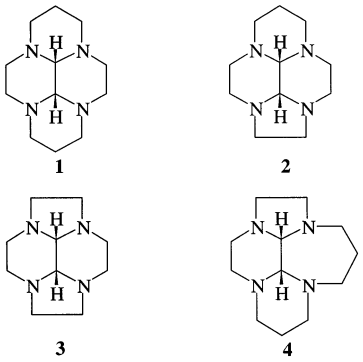

Figure 1. Tetrazamacrocycle−glyoxal condensate ligands **1**−**4**. **1** is derived from cyclam, **2** is derived from [13]aneN4, **3** is derived from cyclen, and **4** is derived from isocyclam.

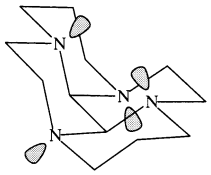

Figure 2. Nitrogen lone pairs of a typical tetraazamacrocycle−glyoxal condensate directed to opposite faces of the molecule in an alternating pattern, resulting in two nonadjacent nitrogens directing their lone pairs into the metal-binding cleft.

aldehyde functional group of glyoxal reacts with two secondary amines of the macrocycle, completing an aminal group and producing a tetracyclic molecule. For both kinetic[8] and thermodynamic reasons,[12] the methine hydrogens of the two-carbon central bridge in the resulting tetracyclic structures are located cis to each other, giving a folded system of four fused rings.[8,9] Trans isomers, which can be obtained for some parent macrocycles, are more nearly flat.[13]

In the usual cis configuration of the tetracyclic bisaminals, the four nitrogen atoms direct their lone pairs to opposite sides of the ligand plane in an alternating pattern. The result is a ligand with two nonadjacent nitrogen lone pairs directed into the concave fold, while the other two nonadjacent nitrogen lone pairs point out from the convex side (Figure 2). It has been suggested that this arrangement might preclude coordination of metal ions by these rigid tetracyclic molecules, since it is sterically impossible for all four nitrogens to bind the same metal ion.[8] However, in a previous study,[14] we found that the two nitrogens with lone pairs converging inside the concave fold of **1** and **3** could bind to Pd^{II} to give the square planar *cis*-dichloro complexes, the first transition metal complexes of this ligand type. Perhaps not surprisingly, these ligands are quite selective, requiring an adequate match in size and geometry with the metal ion; other group 10 ions Ni^{II} and Pt^{II} did not form complexes.[14]

In the Pd^{II} complexes, the rigid tetracycles function as bidentate ligands.[14] Essentially, these ligands behave as very rigid derivatives of ethylenediamine. Copper was chosen to expand the coordination chemistry of these interesting ligands for two reasons: (1) Copper binds amine ligands[15] very strongly. (2) These ligands should provide rigid bidentate donors, a combination that has provided useful model complexes of copper for biomimicry.[1,2]

Experimental Section

Materials. $CuCl_2 \cdot 2H_2O$ (99.9%) and $[Cu(CH_3CN)_4]PF_6$ (99%) were purchased from Aldrich Chemical Co. and used as received. Tetrabutylammonium hexafluorophosphate (>99%) was purchased from Fluka. Cyclam was provided by Procter & Gamble. [13]aneN4 and isocyclam were purchased from the Kansas Advanced Synthetic Laboratory of the University of Kansas. Cyclen was provided by Dow Chemical Co. All solvents were of reagent grade and were dried, when necessary, by accepted procedures.

Physical Techniques. Mass spectra (fast atom bombardment) were obtained using a VG ZAB HS spectrometer equipped with a xenon gun; an NBA (nitrobenzyl alcohol) matrix was used. ESR spectra were recorded on a Bruker ESP 300E spectrometer operating in the X-band. Samples were 0.004 M in 1:1 acetonitrile/toluene saturated with tetrabutylammonium hexafluorophosphate. Electrochemical experiments were performed on a Princeton Applied Research model 175 programmer and model 173 potentiostat using a homemade cell. A glassy carbon electrode was used as the working electrode with a Pt-wire counter electrode and an Ag-wire pseudoreference electrode. All electrochemical measurements were carried out under N_2, on dry, oxygen-free 0.001 M CH_3CN solutions which were 0.1 M in tetrabutylammonium hexafluorophosphate as the supporting electrolyte. The potentials vs SHE were determined using ferrocene as an internal reference. ^1H and ^{13}C NMR spectra were recorded with Bruker DRX400 spectrometer. Electronic spectra were recorded using a Cary 3 spectrophotometer controlled by a Dell Dimension XPS P133s computer. Conductance measurements were performed using a YSI model 35 conductance meter. Elemental analyses were performed by the Analytical Service of the University of Kansas, Desert Analytics, or Quantitative Technologies, Inc.

Synthesis of Ligands. The ligands **1**−**4** were synthesized from the corresponding tetraazamacrocycle according to literature procedures.[9]

Synthesis of $[Cu(L)Cl_2]$ (L = 1−4). The ligand (0.004 mol) was dissolved in 20 mL of methanol. To this stirring solution was added 0.680 g (0.004 mol) of $CuCl_2 \cdot 2H_2O$ dissolved in 10 mL of MeOH. Precipitates ranging from bright green (L = **1**) to dark blue-green (L = **3**), depending on the identity of L, began to form almost immediately. After several hours of stirring, the precipitates were collected by filtration, washed with dry MeOH (5 mL) and then ether (5 mL), and dried in vacuo. Yields: 44% (L = **2**); 64% (L = **4**); 89% (L = **1**); 93% (L = **2**). The FAB^+ mass spectra in methylene chloride (NBA matrix) exhibited no identifiable peaks. Anal. Calcd for Cu(**1**)Cl_2 ($C_{12}H_{22}N_4CuCl_2$): C, 40.40; H, 6.22; N, 15.70. Found: C, 40.38; H, 5.83; N, 15.47. Calcd for Cu(**2**)Cl_2 ($C_{11}H_{20}N_4CuCl_2$): C, 38.55; H, 5.88; N, 16.35. Found: C, 38.25; H, 5.49; N, 16.07. Calcd for Cu(**3**)Cl_2 ($C_{10}H_{18}N_4CuCl_2$): C, 36.54; H, 5.52; N, 17.04. Found: C, 36.30; H, 5.71; N, 16.67. Calcd for Cu(**4**)Cl_2 ($C_{12}H_{22}N_4CuCl_2$): C, 40.40; H, 6.22; N, 15.70. Found: C, 40.15; H, 5.96; N, 15.61. Crystals suitable for X-ray diffraction were grown by the slow diffusion of ether into an acetonitrile solution in all four cases.

Synthesis of $[Cu(3)(\mu\text{-}OH)_2Cu(3)][PF_6]_2 \cdot 1.5H_2O$. To 0.194 g (0.001 mol) of **3** dissolved in 5 mL of acetonitrile, in an inert-

(12) Okawara, T.; Takaishi, H.; Okamota, Y.; Yamasaki, T.; Furukawa, M. *Heterocycles* **1995**, *41*, 1023.
(13) Gluzinski, P.; Krajewski, J. W.; Urbanczyk-Lipkowska, Z.; Bleidelis, J.; Kemme, A. *Acta Crystallogr.* **1982**, *B38*, 3038.
(14) Hubin, T. J.; McCormick, J. M.; Alcock, N. W.; Busch, D. H. *Inorg. Chem.* **1998**, *37*, 6549.
(15) Irving, H.; Williams, R. J. P. *J. Chem. Soc.* **1953**, *Part III*, 3192.

Table 1. Crystal Data and Structural Refinement Details

	Cu(**1**)Cl_2	Cu(**2**)Cl_2	Cu(**3**)Cl_2	Cu(**4**)Cl_2	[Cu(**1**)(μ-OH)$_2$Cu(**1**)]-[PF_6]$_2$·CH_3CN	[Cu(**3**)(μ-OH)$_2$-Cu(**3**)][PF_6]$_2$·2CH_3CN
formula	$C_{12}H_{22}N_4CuCl_2$	$C_{11}H_{20}N_4CuCl_2$	$C_{10}H_{18}N_4CuCl_2$	$C_{12}H_{22}N_4CuCl_2$	$C_{26}H_{49}N_9Cu_2P_2F_{12}O_2$	$C_{24}H_{42}N_{10}Cu_2O_2P_2F_{12}$
fw	356.78	342.75	328.72	356.78	936.755	919.70
cryst syst	orthorhombic	monoclinic	orthorhombic	monoclinic	triclinic	monoclinic
space group	$Pca2_1$	$P2_1/n$	$P2_12_12_1$	$P2_1/c$	$P\bar{1}$	$P2_1/n$
a (Å)	12.9908(5)	8.6548(10)	8.16910(10)	8.6442(10)	10.909(2)	8.1184(2)
b (Å)	6.9267(3)	11.9004(10)	11.59560(10)	13.335(2)	11.713(2)	17.0565(4)
c (Å)	31.9857(13)	13.3657(15)	13.2770(2)	13.1270(5)	8.942(1)	12.9959(3)
$\alpha/\beta/\gamma$ (deg)	−/90/−	−/99.605(5)/−	−/90/−	−/103.398(5)/−	97.11(2)/108.34(2)/113.13(1)	−/101.2730(10)/−
V (Å^3)	2878.2(2)	1357.3(2)	1257.67(3)	1471.9(2)	956.4(4)	1764.84
Z	8	4	4	8	2	2
ρ_{calc} (g/cm^{-3})	1.647	1.677	1.736	1.610	1.70	1.731
temp (K)	180(2)	180(2)	210(2)	200(2)	157(1)	180(2)
abs coeff (mm^{-1})	1.881	1.990	2.144	1.839	3.09	1.401
cryst size (mm)	0.44 × 0.20 × 0.04	0.40 × 0.30 × 0.06	0.35 × 0.15 × 0.15	0.32 × 0.30 × 0.24	0.40 × 0.30 × 0.20	0.25 × 0.25 × 0.04
transm factor range	0.62−0.93	0.7032−0.93	0.61−0.93	0.40−0.89	0.73−1.00	0.67−0.93
max θ (deg)	28.54	28.41	28.42	28.43	108.1	28.53
index ranges	$-14 \le h \le 16$ $-8 \le k \le 6$ $-23 \le l \le 42$	$-7 \le h \le 11$ $-15 \le k \le 15$ $-17 \le l \le 15$	$-10 \le h \le 10$ $-15 \le k \le 14$ $-17 \le l \le 13$	$-9 \le h \le 11$ $-13 \le k \le 17$ $-17 \le l \le 17$	$0 \le h \le 10$ $-11 \le k \le 10$ $-8 \le l \le 8$	$-10 \le h \le 10$ $-22 \le k \le 22$ $-16 \le l \le 11$
no. of reflcns collcd	10 649	7945	7578	8779	2472	10 519
no. of indpt reflcns	4039	3180	2967	3450	2321	4121
no. of obsd reflcns[a]	3368	2063	3502	2269	1881	2445
refinement method	full matrix on F^2	full matrix on F^2	full matrix on F^2	full matrix on F^2	full matrix on F	full matrix on F^2
data/restraint/params	4039/1/343	3180/0/163	2967/0/156	3450/0/172	1881/0/255	4121/34/257
goodness of fit on F^2	0.989	1.009	0.949	0.887	3.56	0.929
R1 indices [$I > 2\sigma(I)$]	0.0297	0.0262	0.0284	0.0436	0.062	0.0515
wR2 indices (all data)[b,c]	0.0685	0.0662	0.0684	0.1012	0.084	0.1479
weight params a, b	0.0378, 0.0000	0.0357, 0.0000	0.0380, 0.0000	0.0450		0.754, 0.0000
largest diff peak and hole (e Å^{-3})	0.407 and −0.412	0.314 and −0.460	0.634 and −0.415	1.3782 and −0.644	0.88 and −0.59	0.891 and −0.741

[a] $I > 2\sigma(I)$. [b] wR1 = $\Sigma||F_o| - |F_c||/|F_o|$. [c] wR2 = $\{\Sigma w(F_o^2 - F_c^2)^2]/\Sigma[w(F_o^2)^2]]^{1/2}$; $w = 1/[s^2(F_o^2) + (aP)^2 + bP]$, where $P = (F_o^2 + 2F_c^2)/3$.

atmosphere glovebox, was added 0.373 g (0.001 mol) of [Cu(CH_3CN)$_4$]PF_6 with stirring. The resulting pale yellow reaction mixture was allowed to stir in the glovebox for 16 h and then removed and stirred in air for an additional 16 h. The solution slowly turned dark blue during this time. After filtration to remove trace solids, the acetonitrile was evaporated to give a dark blue solid. Drying under vacuum yielded 0.367 g, or 85%, of the pure product. The FAB$^+$ mass spectrum in acetonitrile (NBA matrix) exhibited peaks at m/z = 257 (Cu(**3**)$^+$) and m/z = 452 (Cu(**3**)$_2^+$). Anal. Calcd for [Cu(**3**)(μ-OH)$_2$Cu(**3**)][PF_6]$_2$·1.5H_2O ($C_{20}H_{41}N_8Cu_2P_2F_{12}O_{3.5}$): C, 27.72; H, 4.77; N, 12.93. Found: C, 27.80; H, 4.38; N, 12.73. Crystals suitable for X-ray diffraction were grown by the slow diffusion of ether into an acetonitrile solution and contained two acetonitriles of crystallization but did not retain the waters of crystallization present in the bulk solid.

Synthesis of [Cu(1)(μ-OH)$_2$Cu(1)][PF_6]$_2$·MeCN. To 0.444 g (0.002 mol) of **1** dissolved in 10 mL of acetonitrile, in an inert-atmosphere glovebox, was added 0.746 g (0.002 mol) of [Cu(CH_3CN)$_4$]PF_6 with stirring. The resulting pale yellow reaction mixture was allowed to stir in the glovebox for 4 h and then removed and stirred in air for an additional 16 h. The color of the solution slowly changed from pale yellow to green to blue and, finally, to purple during this time. After filtration to remove trace solids, the acetonitrile was evaporated to give a brown solid. Drying under vacuum yielded 0.615 g, or 66%, of the pure product. The FAB$^+$ mass spectrum in THF (NBA matrix) exhibited a small peak at m/z = 604 (Cu$_2$(**3**)$_2O_2^+$). Anal. Calcd for [Cu(**1**)(μ-OH)$_2$Cu(**1**)]-[PF_6]$_2$·MeCN ($C_{26}H_{49}N_9Cu_2P_2F_{12}O_2$): C, 33.34; H, 5.27; N, 13.46. Found: C, 33.66; H, 5.06; N, 13.31. Dark purple crystals suitable for X-ray diffraction were grown by the slow diffusion of ether into an acetonitrile solution.

X-ray Crystallography. X-ray data were collected with a Siemens SMART[16] three-circle system with CCD area detector using graphite-monochromated Mo Kα radiation (λ = 0.710 71 Å). The crystals were held at the specified temperature with the Oxford Cryosystem Cooler.[17] Absorption corrections were applied by the Ψ-scan method, and none of the crystals showed any decay during data collection. The X-ray data for [Cu(**1**)(μ-OH)$_2$Cu(**1**)][PF_6]$_2$·MeCN were obtained with a Rigaku AFC5R diffractometer with graphite-monochromated Cu Kα radiation and a rotating anode generator. For this crystal, an empirical absorption correction based on azimuthal scans of several reflections was applied which resulted in transmission factors ranging from 0.73 to 1.00. The data were corrected for Lorentz and polarization effects. A correction for secondary extinction was applied (coefficient = 1.364 21 × 10^{-6}).

The structures were solved by direct methods using SHELXS[18] (TREF) with additional light atoms found by Fourier methods. Hydrogen atoms were added at calculated positions and refined using a riding model. Anisotropic displacement parameters were used for all non-H atoms, while H-atoms were given isotropic displacement parameters equal to 1.2 (or 1.5 for methyl hydrogen atoms) times the equivalent isotropic displacement parameter for the atom to which the H-atom is attached. Refinement used SHELXL 96.[19] The structure of [Cu(**1**)(μ-OH)$_2$Cu(**1**)][PF_6]$_2$·MeCN was solved by direct methods (SIR92)[20] and expanded using Fourier techniques (DIRDIF94).[21] The non-hydrogen atoms were refined anisotropically.

Table 1 holds crystal data and refinement details for the six new structures appearing in this paper. Selected bond lengths and angles can be found in Table 2.

Results and Discussion

Synthesis of Complexes. As described in the Introduction, the first metal ion derivatives to be characterized for these

(16) *SMART User's manual*; Siemens Industrial Automation Inc: Madison, WI, 1995.
(17) Cosier, J.; Glazer, A. M. *J. Appl. Crystallogr.* **1986**, *19*, 105.
(18) Sheldrick, G. M. *Acta Crystallogr.* **1990**, *A46*, 467.
(19) Sheldrick, G. M. *SHELX-96 (beta-test) (including SHELXS and SHELXL)*; University of Gottingen: Gottingen, Germany, 1996.
(20) Altomare, A.; Cascarano, M.; Giacovazzo, C.; Guagliardi, A. *J. Appl. Crystallogr.* **1993**, *26*, 343.
(21) Beurskens, P. T.; Admiraal, G.; Beurskens, G.; Bosman, W. P.; de Gelder, R.; Israel, R.; Smits, J. M. M. *The DIRDIF-94 program system*; Technical Report of the Crystallographic Laboratory: University of Nijmegen, Nijmegen, The Netherlands, 1994.

Table 2. Selected Bond Lengths (Å) and Angles (deg)

(i) Cu(**1**)Cl_2

Cu(1)−N(18)	2.083(5)	Cu(2)−N(21)	2.098(6)
Cu(1)−N(11)	2.099(6)	Cu(2)−N(28)	2.107(4)
Cu(1)−Cl(11)	2.2248(13)	Cu(2)−Cl(21)	2.2303(14)
Cu(1)−Cl(12)	2.2404(13)	Cu(2)−Cl(22)	2.2388(13)
N(18)−Cu(1)−N(11)	84.8(2)	N(21)−Cu(2)−N(28)	84.6(2)
N(18)−Cu(1)−Cl(11)	159.48(15)	N(21)−Cu(2)−Cl(21)	93.8(2)
N(11)−Cu(1)−Cl(11)	93.0(2)	N(28)−Cu(2)−Cl(21)	159.53(14)
N(18)−Cu(1)−Cl(12)	93.47(14)	N(21)−Cu(2)−Cl(22)	158.90(15)
N(11)−Cu(1)−Cl(12)	159.80(17)	N(28)−Cu(2)−Cl(22)	93.13(15)
Cl(11)−Cu(1)−Cl(12)	95.36(5)	Cl(21)−Cu(2)−Cl(22)	95.44(5)

(ii) Cu(**2**)Cl_2

Cu(1)−N(1)	2.0683(16)	Cu(1)−Cl(2)	2.2394(6)
Cu(1)−N(7)	2.0903(15)	Cu(1)−Cl(1)	2.2407(5)
N(1)−Cu(1)−N(7)	84.03(6)	N(1)−Cu(1)− Cl(1)	90.62(4)
N(1)−Cu(1)−Cl(2)	168.19(5)	N(7)−Cu(1)− Cl(1)	165.96(5)
N(7)−Cu(1)−Cl(2)	91.52(5)	Cl(2)−Cu(1)− Cl(1)	96.08(2)

(iii) Cu(**3**)Cl_2

Cu(1)−N(1)	2.070(2)	Cu(1)−Cl(1)	2.2277(7)
Cu(1)−N(7)	2.072(2)	Cu(1)−Cl(2)	2.2315(6)
N(1)−Cu(1)−N(7)	83.33(8)	N(1)−Cu(1)−Cl(2)	90.96(5)
N(1)−Cu(1)−Cl(1)	169.43(6)	N(7)−Cu(1)−Cl(2)	168.76(6)
N(7)−Cu(1)−Cl(1)	92.07(6)	Cl(1)−Cu(1)−Cl(2)	95.11(3)

(iv) Cu(**4**)Cl_2

Cu(1)−N(8)	2.095(3)	Cu(1)−Cl(1)	2.2261(9)
Cu(1)−N(12)	2.098(2)	Cu(1)−Cl(2)	2.2447(9)
N(8)−Cu(1)−N(12)	78.28(9)	N(8)−Cu(1)−Cl(2)	97.58(7)
N(8)−Cu(1)−Cl(1)	156.30(8)	N(12)−Cu(1)−Cl(2)	144.94(8)
N(12)−Cu(1)−Cl(1)	98.22(7)	Cl(1)−Cu(1)−Cl(2)	98.27(3)

(v) [Cu(**3**)(μ-OH)$_2$Cu(**3**)]$^{2+}$

Cu(1)−O(1)	1.923(3)	Cu(1)−N(7)	2.047(3)
Cu(1)−N(1)	2.044(3)		
O(1)−Cu(1)−O(1)#1	81.36(12)	O(1)#1−Cu(1)−N(7)	170.58(13)
O(1)−Cu(1)−N(1)	171.74(13)	N(1)−Cu(1)−N(7)	84.66(13)
O(1)−Cu(1)−N(7)	97.55(12)	Cu(1)−O(1)−Cu(1)#1	98.64(12)

(vi) [Cu(**1**)(μ-OH)$_2$Cu(**1**)]$^{2+}$

Cu(1)−O(1)	1.911(4)	Cu(1)−N(1)	2.054(4)
Cu(1)−N(8)	2.047(4)		
O(1)−Cu(1)−O(1)*	80.1(2)	O(1)−Cu(1)− N(8)	96.8(2)
O(1)−Cu(1)−N(1)	173.1(2)	N(1)−Cu(1)−N(8)	86.7(2)
O(1)−Cu(1)−N(8)*	175.8(2)	Cu(1)−O(1)−Cu(1)	99.9(2)

tetracyclic bisaminal ligands were Pd^{II} complexes of **1** and **3**.[14] Attempts to synthesize complexes with other group 10 ions, Ni^{II} and Pt^{II}, failed. To expand the range of their metal complexes and to help understand the apparent selectivity of these ligands, Cu^{I} was chosen for study. It is relatively soft, like Pd^{II}, and has a similar ionic radius (74 and 78 pm, respectively, in their four-coordinate complexes),[22] though its preferred coordination geometry is tetrahedral rather than square planar geometry.

Complexation reactions of [Cu(CH_3CN)$_4$]PF_6 with ligands **1** and **3** were performed in acetonitrile under an inert atmosphere. Initial characterization of the resulting colorless products was promising, as mass spectral and NMR data showed evidence of complex formation. Unfortunately, the isolation of pure Cu^{I} complexes proved difficult. In the case of **1**, colorless crystals can be obtained by slow evaporation of the acetonitrile solvent from the reaction solution under nitrogen. Close examination, however, revealed at least two distinct crystal types, and the ^{1}H NMR spectrum of this sample indicated at least two different environments for the ligand protons. Fortunately, the X-ray crystal structure[23] of one crystal type was obtained, demonstrating that a Cu^{I} complex did indeed form. Surprisingly, the complex contained two molecules of **1**, each coordinated to a central Cu^{I} ion by a single, inward-facing nitrogen of the folded ligand (Figure 3).[23] Although the second inward-facing nitrogen atom of each ligand is oriented appropriately for binding, the Cu···N distances are about 0.4 Å longer than the bound Cu−N distances. Clearly, the steric bulk of **1** forces this geometry when two ligands coordinate to the same metal ion. Separation of the other crystalline product has not proved possible, so [Cu(**1**)$_2$]PF_6 has not been further characterized.

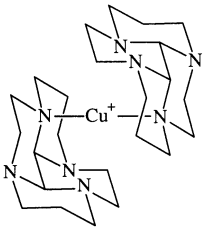

Figure 3. Structure of a Cu^{I} bis-**1** complex in which only one nitrogen of each ligand binds the metal ion.[23]

With ligand **3**, the same Cu^{I} complexation reaction also results in a mixture of products, which have not been characterized. However, air oxidation of the crude Cu^{I} reaction mixture results in the formation of a dark blue solution, which ultimately yields a blue solid analyzing as the Cu^{II}(**3**) bis(μ-hydroxo) dimer. An X-ray crystal structure of crystals grown from ether diffusion into an acetonitrile solution confirms this formulation, a common one for synthetic copper complexes.[3−6,24−28] Oxidation by air of the Cu^{I}−ligand **1** product mixture in MeCN also causes a color change, this time to a purple solution, signifying an oxidation state change for the copper. Elemental analysis of the brown solid obtained upon solvent evaporation shows this product to be the analogous bis(μ-hydroxo) dimer of ligand **1**. X-ray-quality purple crystals were obtained by the slow diffusion of ether into an acetonitrile solution of this material, and the resulting structure confirms the formulation (below).

Because of the difficulties encountered in isolating the pure Cu^{I} complexes, and because the dimer structures indicated that Cu^{II} can coordinate to these ligands, we examined the complexes of Cu^{II} further. Methanol solutions of each of the ligands **1**−**4** were mixed in air with 1 equiv of $CuCl_2$·$2H_2O$. From these reactions, pure complexes of formula $CuLCl_2$ (L = **1**−**4**) were isolated as powdered samples that gave good elemental analyses, with none of the difficulties that

(22) Huheey, J. E.; Keiter, E. A.; Keiter, R. L. *Inorganic Chemistry: Principles of Structure and Reactivity*, 4th ed.; HarperCollins: New York, 1993.

(23) Hubin, T. J.; Alcock, N. W.; Clase, H. J.; Busch, D. H. *Acta Crystallogr., Sect. C* **1999**, *55*, 1402.

(24) Davies, G.; El-Sayed, M. A. *Comments Inorg. Chem.* **1985**, *4*, 151.

(25) Davies, G.; El-Sayed, M. A. *Inorg. Chem.* **1983**, *22*, 1257.

(26) Caulton, K. G.; Davies, G.; Holt, E. M. *Polyhedron* **1990**, *9*, 2319.

(27) Sanyal, I.; Mahroof-Tahir, M.; Nasir, M. S.; Ghosh, P.; Cohen, B. I.; Gultneh, Y.; Cruse, R. W.; Farooq, A.; Karlin, K. D.; Liu, S.; Zubieta, J. *Inorg. Chem.* **1992**, *31*, 4322.

(28) Lee, D.-H.; Murthy, N. N.; Karlin, K. D. *Inorg. Chem.* **1996**, *35*, 804.

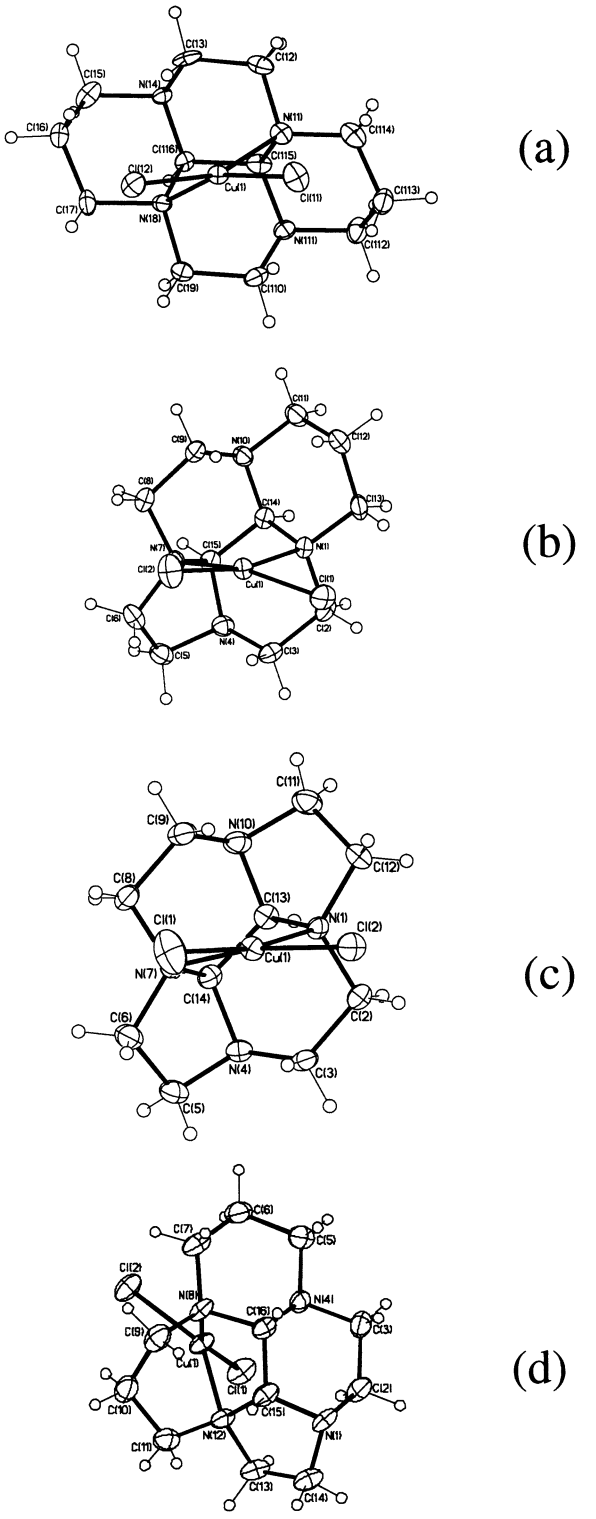

Figure 4. Representations of the crystal structures of (a) Cu(**1**)Cl_2, (b) Cu(**2**)Cl_2, (c) Cu(**3**)Cl_2, and (d) Cu(**4**)Cl_2.

had frustrated work on the Cu^I systems. The complexes are highly colored, ranging from a bright green to dark blue-green.

Crystal Structures. The crystal structures of Cu(**1**)Cl_2, Cu(**2**)Cl_2, Cu(**3**)Cl_2, and Cu(**4**)Cl_2 are shown in Figure 4 a−d, and those of the bis(μ-hydroxo) dimers of Cu(**3**) and Cu(**1**), in Figure 5 a,b. All have four-coordinate Cu^{II} ions bound to two nitrogens of a single bidentate tetracyclic ligand. In the

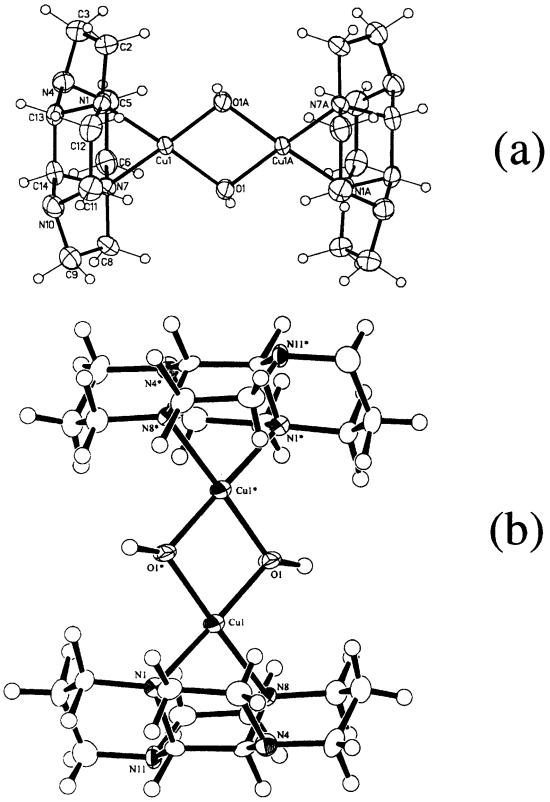

Figure 5. Synthesis of cross-bridged tetraazamacrocycles requiring selective alkylation of nonadjacent nitrogens of tetraazamacrocycle−glyoxal condensates.[29,30]

monomers, the coordination spheres are completed by *cis*-chloro ligands, while, in the dimers, the last two ligands for both Cu^{II} ions are bridging μ-hydroxo anions, resulting in the familiar Cu_2O_2 diamond-shaped core.[3−6,24−28]

Of the four monomers, the most striking feature is the unique coordination mode of **4**. The other three complexes feature four-coordinate Cu^{2+} bound to two, nonadjacent, inward-facing nitrogens of the bidentate tetracycle and to two chloro ligands (Figure 4a−c). These structures are very similar to the Pd^{2+} structures previously determined.[14] However, **4** binds to Cu^{II} through two adjacent nitrogen atoms of the tetracyclic bisaminals (Figure 4d). This is the first glyoxal−tetraazamacrocycle condensate to show this coordination mode, and the distinctive coordination mode probably results from the asymmetry of the parent 14-membered isocyclam ring. The two adjacent trimethylene chains are absent from the more symmetric cyclam, [13]-aneN4, and cyclen macrocycle parents of ligands **1**−**3**, respectively. In the complex, the isocyclam−glyoxal condensate, **4**, has a conformation unlike those of ligands **1**−**3**. In the latter, the *cis*-methine hydrogens and the symmetrically arranged five- and six-membered fused rings result in only two nonadjacent nitrogens directing their lone pairs into the fold. With **4**, however, the same *cis*-methine conformation, coupled with the asymmetric arrangement of five-, six-, and seven-membered fused rings results in three nitrogens directing their lone pairs into the fold, leaving only one pointing out from the convex side. Only two of these inward-facing nitrogens bind Cu^{II}, and they are adjacent to one another, members of the same seven-membered ring. This

seven-membered ring is the only one found in any of the four ligands and rationalizes the distinctiveness of **4**.

The structure of Cu(**4**)Cl_2 makes it clear why **4** has a different reactivity from that of **1**−**3**, as well as its conformational uniqueness. **1**−**3** are useful precursors for the generation of cross-bridged tetraazamacrocycles because they are selectively dialkylated at nonadjacent nitrogens (Figure 6).[29−31] In contrast, **4**[32] and the glyoxal condensate of [15]-aneN4[33] do not give cross-bridged ligands by the Weisman route.[29−31] Perhaps these syntheses fail because of the seven-membered rings in both tetracycles, whose flexibility destroys the necessary concave−convex alternation of reactive nitrogen atoms. Alkylation of these tetracycles does not give the nonadjacent dialkylated product; thus, no cross-bridged ligand is produced by further reaction, as for **1**−**3**.

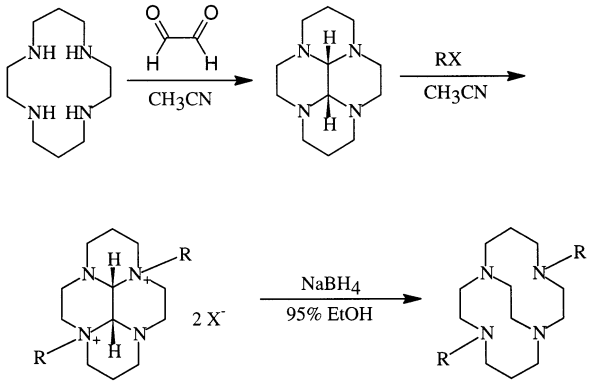

Figure 6. Representations of the crystal structures of (a) [Cu(**3**)(μ-OH)$_2$Cu(**3**)]$^{2+}$ and (b) [Cu(**1**)(μ-OH)$_2$Cu(**1**)]$^{2+}$.

A more subtle difference in the Cu^{II} structures is the coordination geometry around Cu^{II}. As the parent ring size of the tetracycle increases, the coordination polyhedron around Cu^{II} becomes more distorted, moving away from square planar to a geometry intermediate between tetrahedral and square planar. A comparison of the improper torsion angles, the angles formed by the Cu−N bond and its projection onto the Cl−Cu−Cl (or O−Cu−O) plane, illustrates this trend. For a square planar complex, this angle would be 0°, while, for a tetrahedral complex, it would be 54.5° (half of the 109° tetrahedral bond angle). In the dimeric complex (vide infra) derived from the 12-membered ligand (L = **3**), this angle averages 8.80° (all bound nitrogens are approximately coplanar, with the Cu_2O_2 plane offset by this same angle), while, in the corresponding monomer, it is 8.66° for both nitrogens. In the Cu(II) derivative of 13-membered **2**, this angle grows to an average of 10.78° and is even larger, averaging 18.78°, for the monomer complex of 14-membered ligand **1**. Yet this angle averages only 3.96° in the dimer of ligand **1** (vide infra). Finally, in the complex of the asymmetric isocyclam derived ligand **4**, these two angle are quite different for the two bound nitrogen atoms: 17.52 and 30.70°, respectively. The asymmetry in Cu(**4**)Cl_2 comes about because the two bound nitrogens are adjacent to each other. Comparisons of the derivatives of this ligand with those of the other ligands must be made with caution, since we have seen that a different binding mode exists here. In the other complexes, the angles for the two bound nitrogens do not differ by more than 2°.

Why do the larger ligands force a geometric distortion away from the square planar structure favored by Cu^{II} ion toward tetrahedral? Their steric bulk is the probable cause. It is important to observe that the shallow cleft in these folded ligands lies approximately perpendicular to the N−Cu−N plane. Putting the two chloro ligands in the remaining square planar positions causes steric interference with the periphery of the folded tetramine. Since the cleft lies at a right angle to the chloro positions, the chlorides are forced to align with it to ease the steric interaction, producing a distortion toward tetrahedral geometry. This distortion is more pronounced in the larger ligand complexes because their greater bulk increases the steric interactions. Cu(**4**)Cl_2 has one chloro ligand particularly distorted from the square planar position because its adjacent bound nitrogens force the ligand periphery even closer to this chloride, while the other chloride is free to occupy the majority of the ligand cleft and its position is less affected. Of note is the small improper distortion angle of the ligand **1** dimer (3.96°). Apparently this near square planar geometry is allowed by the smaller (than chloride) oxygen ligands even though the ring size trend would predict a larger distortion toward tetrahedral. The geometry intermediate between square planar and tetrahedral that results from the ligand conformations is often noted[34] as a special adaptation of blue copper electron-transfer protein active sites. By providing a low-energy barrier to reorganization, those enzymes support electron transfer between Cu^{II} (preferring square planar coordination) and Cu^{I} (preferring tetrahedral coordination).

Finally, the dimeric complexes formed between Cu^{II} and ligands **1** and **3** must be discussed (Figure 5). The oxygenation of Cu^{I} complexes to μ-oxo- or μ-hydroxo-bridged Cu^{II} or Cu^{III} dimers is common in synthetic inorganic chemistry.[3−6,24−28] The generally accepted mechanism for this transformation is, first, the formation of a peroxodicopper(II) species, followed by O−O bond cleavage induced by other Cu^{I} ions acting as electron donors. Since no mechanistic studies have yet been carried out on the formation of the present dimers, literature examples must be used to rationalize the present system. It should be pointed out that the dinuclear complexes may exist in diastereomeric forms, since the ligands occur as enantiomers. Investigations focusing on the affects of ligand chirality have not been attempted.

The available X-ray crystal structures do not provide locations for the protons on the bridging hydroxo ligands,

(29) Weisman, G. R.; Rogers, M. E.; Wong, E. H.; Jasinski, J. P.; Paight, E. S. *J. Am. Chem. Soc.* **1990**, *112*, 8604.
(30) Weisman, G. R.; Wong, E. H.; Hill, D. C.; Rogers, M. E.; Reed, J. P.; Calabrese, J. C. *J. Chem. Soc., Chem. Commun.* **1996**, 947.
(31) Wong, E. H.; Weisman, G. R.; Hill, D. C.; Reed, D. P.; Rogers, M. E.; Condon, J. S.; Fagan, M. A.; Calabrese, J. C.; Lam, K.-C.; Guzei, I. A.; Rheingold, A. L. *J. Am. Chem. Soc.* **2000**, *122*, 10561.
(32) Perkins, C. M. Private communication, 1998.
(33) Collinson, S. R.; Hubin, T. J.; Alcock, N. W.; Busch, D. H. *J. Coord. Chem.* **2001**, *52*, 317.
(34) Holm, R. H.; Kennepohl, P.; Solomon, E. I. *Chem. Rev.* **1996**, *96*, 2239 and references therein.

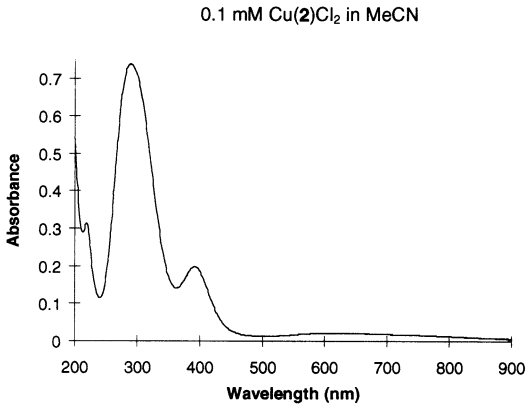

Figure 7. Electronic spectrum of Cu(**2**)Cl_2 representative of the spectra of all four monomeric complexes. Table 3 contains the pertinent data.

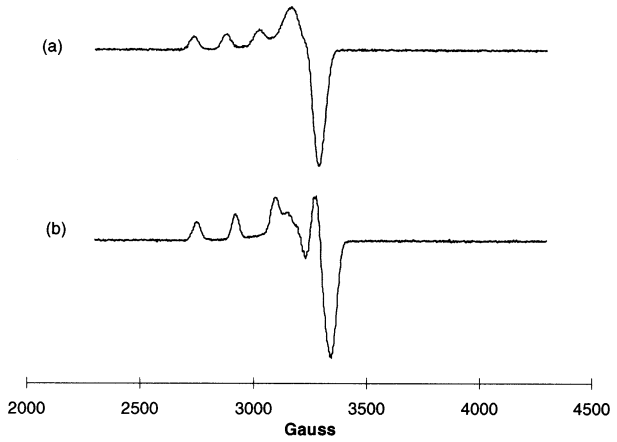

Figure 8. EPR spectra of (a) Cu(**4**)Cl_2 distinct from the three L = **1**−**3** complexes, whose spectra are exemplified by that of (b) Cu(**1**)Cl_2. The complexes were 0.004 M in 1:1 acetonitrile/toluene saturated with tetrabutylammonium hexafluorophosphate.

but comparison of bond lengths with literature examples[3−6,24−28] indicates that the structures are best assigned as dicopper(II)−bis(μ-hydroxo) species rather than dicopper(III)−bis(μ-oxo) species. For the ligand **3** dimer Cu−O = 1.923(3) and 1.925(3) Å and Cu−N = 2.044(3) and 2.047(3) Å. The Cu···Cu distance is 2.918 Å, while the O···O distance is 2.508 Å. The core bond angles are Cu−O−Cu = 98.64(12)° and O−Cu−O = 81.36(12)°. For the ligand **1** dimer Cu−O = 1.911(4) and 1.907(4) Å, Cu−N = 2.054(4) and 2.047(4) Å, Cu···Cu = 2.925 Å, and O···O = 2.439 Å. The core bond angles are Cu−O−Cu = 99.9(2)° and O−Cu−O = 80.1(2)°. These metrical parameters are very similar to other synthetic complexes having the dicopper(II)−bis(μ-hydroxo) core, such as Kitajima's tris(pyrazolyl)borate complexes with typical Cu···Cu distances of 2.937−3.059 Å and similar Cu−O−Cu bond angles[3,4] or Tolman's triazacyclononane complexes with typical Cu···Cu distances of 2.977−3.037 Å and again similar Cu−O−Cu bond angles.[5] The parameters are also similar to those for the oxidized form of catechol oxidase where the Cu···Cu distance is 2.87 Å.[35] As rigid bidentate ligands have been shown to form important model complexes for O_2 activation by Cu metalloenzymes,[1,2] the mechanism of dimer formation in these cases, and the isolation of intermediates arising from oxidation of Cu^+ complexes of the present ligands, are worthy of further investigation.

Electronic Structure. The magnetic moments of the $CuLCl_2$ complexes are all typical of such Cu^{II} derivatives:[20] μ_{eff} = 1.96 μ_B for Cu(**1**)Cl_2; μ_{eff} = 1.82 μ_B for Cu(**2**)Cl_2; μ_{eff} = 1.81 μ_B for Cu(**3**)Cl_2; μ_{eff} = 1.91 μ_B for Cu(**1**)Cl_2. These values indicate no strong ferromagnetic or antiferromagnetic coupling in the bulk solids. The unsymmetric Cu(**4**)Cl_2 complex also shows no significantly different magnetic properties.

The electronic spectra of the monomeric complexes (Figure 7) all exhibit several intense broad absorptions from 200 to 400 nm, common to LMCT bands for Cu^{II} species (see Table 3). Assignment of the bands is difficult, but the higher energy ones are likely due to $\sigma-\sigma^*$ transitions from the tertiary amino or chloro ligands, while the less intense, lower energy band near 400 nm is more likely to arise from a $\pi-\pi^*$ transition from the chloro ligands.[36] The d−d transitions of these complexes are broad, with only one maximum found below 900 nm. The present complexes exhibit a trend consistent with the literature: as a family of tetrahedral Cu^{II} complexes flattens out toward a square planar geometry, the d−d bands tend to shift toward higher energies.[36] As the improper torsion angle decreases (toward 0° at square planar), the d−d bands move to increasingly shorter wavelengths (higher energies): Cu(**4**)Cl_2 angle averages 24.11°, d−d band = 712 nm; Cu(**1**)Cl_2 angle averages 18.78°, d−d band = 653 nm; Cu(**2**)Cl_2 angle averages 10.78°, d−d band = 637 nm; Cu(**3**)Cl_2 angle averages 8.66°, d−d band = 638 nm (see Table 3). The last two complexes, of ligands **2** and **3**, do not show much difference in the wavelengths of their d−d bands, but their improper torsion angles are also not very different.

Table 3. Electronic Spectra of Cu^{II} Monomer Complexes in Acetonitrile

complex	charge-transfer bands	d−d band (nm) (extinctn coeff (M^{-1} cm^{-1}))
Cu(**1**)Cl_2	220 sh (2520), 285 (4530), 399 (1090)	653 (90)
Cu(**2**)Cl_2	219 (3130), 289 (7390), 392 (1980)	637 (140)
Cu(**3**)Cl_2	220 (2490), 293 (5560), 388 (1490)	638 (100)
Cu(**4**)Cl_2	215 sh (3340), 236 sh (1480), 287 (5940), 378 (1520)	712 (180)

EPR spectra of the monomeric complexes in frozen 1:1 MeCN/toluene solutions are shown in Figure 8. The signals are familiar for Cu^{II} complexes but appear to have some rhombic character. In the absence of simulation studies, the Hamiltonian parameters have not been calculated. However, some conclusions can be drawn from a qualitative analysis of the spectra. Clearly, ligand **4** imparts a unique environment on the paramagnetic Cu^{II} ion in frozen solution (Figure 8a), corresponding to its unique solid-state structure. The EPR spectrum of Cu(**4**)Cl_2 differs from the other three complexes in its more Gaussian peaks, lacking a shoulder between what would normally be described as the $g_{||}$ and the g_z absorptions

(35) Klabunde, T.; Eicken, C.; Sacchettini, J. C.; Krebs, B. *Nat. Struct. Biol.* **1998**, *5*, 1084.

(36) Lever, A. B. P. *Inorganic Electronic Spectroscopy*, 2nd ed.; Elsevier: Amsterdam, 1984.

Table 4. Molar Conductance of Cu^{II} Chloride Complexes in Various Solvents[a]

complex	acetonitrile	DMF	methanol
Cu(**1**)Cl_2	2.50	14.9	76.5
Cu(**2**)Cl_2	4.70	9.90	57.8
Cu(**3**)Cl_2	22.2	14.4	50.0
Cu(**4**)Cl_2	6.20	9.60	67.1
1:1	120−160	65−90	75−95
2:1	220−300	130−170	150−180

[a] Theoretical conductance values from ref 34.

and lacking fine structure in the $g_{||}$ absorption. The complexes of **1**−**3** give EPR spectra that are nearly identical, exemplified by the spectrum of Cu(**1**)Cl_2 in Figure 8b.

Solution Properties. The molar conductances of the four monomeric complexes were measured in 1 mM solutions (Table 4), to determine the ability of solvent to replace the chloro ligands.[37] Results were obtained for acetonitrile, DMF, and methanol solutions, but lack of solubility prevented parallel aqueous experiments. These data indicate that in the least coordinating solvent, acetonitrile, the complexes remain intact; no solvent molecules replace chloro ligands, and the complexes are nonelectrolytes. In DMF, a somewhat better coordinating solvent with a similar dielectric constant, the complexes are still characterized by nonelectrolyte behavior. In MeOH however, an even better coordinating solvent with slightly lower dielectric constants, the complexes all behave nearly as 1:1 electrolytes, indicating that one chloro ligand is almost fully replaced by solvent. Probably the important quality of methanol is its ability to solvate the chloride anion by hydrogen bond formation. This should greatly favor ionization.

Cyclic voltammograms of the $CuLCl_2$ complexes were obtained with a glassy carbon working electrode in 1 mM acetonitrile solutions containing 0.1 M tetrabutylammonium hexafluorophosphate. All four complexes showed a direction dependence in their cyclic voltammograms. Initial scanning in the positive direction resulted in no oxidation waves being detected and only a single observable irreversible reduction. However, if the single cycle scan was started in the negative direction (or several cycles were carried out, beginning in the positive direction), a return oxidation wave was present (Figure 9). We interpret this phenomenon as follows: oxidation of the intact (see conductance data above) $CuLCl_2$ complex to a Cu^{III} derivative is not favored in acetonitrile, but one-electron reduction of this complex to Cu^{I} does take place. The likely loss of one or more negatively charged chloro ligands from the univalent copper ion causes the return oxidation of the new Cu^{I} species to occur at a much higher potential than for the original species. This change in coordination number would be expected to produce an irreversible electrode couple. Clearly, the oxidation wave is dependent on the prior reduction to produce the oxidizable species. The in situ generated Cu^{I} species may be formulated as $CuL(MeCN)_x^+$.

(37) (a) Angelici, R. J. *Synthesis and Techniques in Inorganic Chemistry*; University Science Books: Mill Valley, CA, 1986; Appendix 2. (b) Feltham, R. D.; Hayter, R. G. *J. Chem. Soc.* **1964**, 4587. (c) Geary, W. J. *Coord. Chem. Rev.* **1971**, *7*, 81.

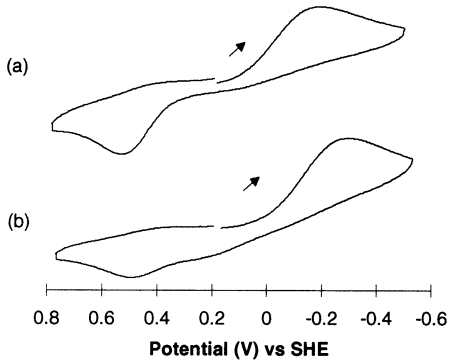

Figure 9. Cyclic voltammograms of (a) Cu(**3**)Cl_2 and (b) Cu(**1**)Cl_2 show the irreversible reduction and its return oxidation. The complexes were 0.001 M in acetonitrile.

Table 5. Cyclic Voltammetry of Cu^{II} Monomer Complexes in Acetonitrile

complex	E_{red} (V) vs SHE	E_{ox} (V) vs SHE
Cu(**1**)Cl_2	−0.175	+0.505
Cu(**2**)Cl_2	−0.218	+0.501
Cu(**3**)Cl_2	−0.195	+0.530
Cu(**4**)Cl_2	−0.301	+0.494

Although this pattern is observed for all four complexes, the structural uniqueness of Cu(**4**)Cl_2 is again evident. While the return oxidation for the L = **1**−**3** complexes all have a similar shape and intensity, the oxidation of Cu(**4**)Cl_2 draws much less current and has a small shoulder at a lower potential, possibly indicating that multiple Cu^{I} complexes are in equilibrium after their in situ formation. The initial reduction potential for this species is also approximately 100 mV more cathodic than those for the more similar L = **1**−**3** complexes, indicating that its geometry stabilizes Cu^{II} compared to the other ligands. This fact is surprising in view of the Cu(**4**)Cl_2 structure, which is the most distorted toward tetrahedral, a geometry favored by Cu^{I}. However, the unique binding of adjacent ligand nitrogens in **4** may explain this inconsistency. These nitrogens may be too close together in their seven-membered ring or otherwise less well positioned (compared to the nonadjacent bound nitrogens in **1**−**3**) to stabilize the larger Cu^{I} ion. It is also possible that the third concave facing nitrogen (N(4), Figure 4d) may be able to coordinate to copper(I) after this ion is produced by the reduction. The irreversible reduction and oxidation potentials for all four complexes are given in Table 5.

Conclusions

We have shown for the first time that Cu^{2+} forms coordination compounds having the general formula $Cu(L)Cl_2$ with a range of tetraazamacrocycle−glyoxal condensates. The X-ray crystal structures of five such complexes reveal that the ligands are bidentate in all cases, with **1**−**3** binding through nonadjacent, concave facing nitrogens, as was previously found for the Pd^{II} coordination of **1** and **3**.[14] Ligand **2** was structurally characterized for the first time in its Cu^{II} complex and was shown to have a folded conformation similar to that of **1** and **3**, all of which have a cleft where the metal ion binds. The ligand **4** was also structurally characterized for the first time, here as a bidentate ligand in

its Cu^{II} complex. This structure shows **4** to have three concave-facing nitrogens and a much broader cleft for metal ion binding. Only two of the nitrogens bind Cu^{II}; they are adjacent in the parent macrocycle ring and members of the same seven-membered ring in the glyoxal condensate—both properties are unique to this ligand as compared to **1**−**3**. The structure provides an explanation for why the Weisman-type[27,28] cross-bridging of isocyclam is unsuccessful: the pivotal trans dialkylation step (seen in **1**−**3**) of the tetracyclic precursor, **4**, does not occur regioselectively because the orientation of the reactive nitrogen atoms is evidently unfavorable. The electronic properties of the complexes are rather typical of four-coordinate copper(II). However, the unique geometry of Cu(**4**)Cl_2 is evident in its distinct EPR spectrum. The monomeric complexes all display irreversible Cu^{II}/Cu^{I} couples in acetonitrile. Again, the behavior of Cu(**4**)-Cl_2 is slightly different from that of the L = **1**−**3** complexes. Finally, we have shown that the Cu^{II} bis(μ-hydroxo) dimer of ligand **3** can form from reaction of the Cu^{I} complex (formed in situ) with air. The X-ray crystal structure reported is typical for such dimers and indicates that the rigid bidentate ligands presented here may be useful for modeling dicopper enzyme active sites.

Acknowledgment. The generous support of this work by the Procter & Gamble Co. is greatly appreciated. T.J.H. thanks the Madison and Lila Self-Graduate Research Fellowship of the University of Kansas for financial support. We thank EPSRC and Siemens Analytical Instruments for grants in support of the diffractometer. The Kansas/Warwick collaboration has been supported by NATO.

Supporting Information Available: A total of 23 tables of bond distances and angles, anisotropic displacement parameters, hydrogen coordinates, and isotropic displacement parameters for Cu(**1**)Cl_2, Cu(**2**)Cl_2, Cu(**3**)Cl_2, Cu(**1**)Cl_2, [Cu(**3**)(μ-OH)$_2$Cu(**3**)]-$[PF_6]_2$, and [Cu(**1**)(μ-OH)$_2$Cu(**1**)]$[PF_6]_2$. This material is available free of charge via the Internet at http://pub.acs.org.

IC020386+